Linear and nonlinear viscoelasticity of oleogels based on vegetable oil and ethylene vinyl acetate copolymer/isotactic polypropylene blends

Jose Enrique Martín Alfonso,[1,2] Concepción Valencia[1,2]

[1]Departamento de Ingeniería Química, Química Física y Química Orgánica. Campus de "El Carmen," Universidad de Huelva, 21071 Huelva, Spain
[2]Pro2TecS – Chemical Process and Product Technology Research Center, 21071 Huelva, Spain
Correspondence to: J. E. Martín-Alfonso (E-mail: jose.martin@diq.uhu.es)

ABSTRACT: This work deals with a rheological study of oleogels based on high-oleic sunflower oil (HOSO) and ethylene vinyl acetate copolymer (EVA) / isotactic polypropylene (iPP) blends. EVA copolymers with different vinyl acetate content were used. With this aim, linear small amplitude oscillatory shear (SAOS) and nonlinear (relaxation) measurements combined with polarized optical microscopy were carried out. Oleogels were prepared by using the mixing rheometry technique in a batch mixer. Oscillatory strain amplitude sweep tests showed that the end from the viscoelastic linear region for oleogels was accompanied by opposite trends for viscoelastic moduli. SAOS tests showed that all the oleogels present similar behavior characteristic of polymeric systems with physical entanglements. It was found that the elastic equilibrium modulus and loss tangent increases with iPP content. On the other hand, nonlinear relaxation tests presented a strong dependence on the strain applied and the Soskey–Winter model was found to provide an accurate description of the damping function of these oleogels. © 2015 Wiley Periodicals, Inc. J. Appl. Polym. Sci. **2015**, *132*, 42477.

INTRODUCTION

Oleogels are generally highly structured colloidal dispersions, consisting of a gelling agent dispersed in liquid oil medium.[1] The gelling agent is generally a low molecular-weight organic molecules or polymers, which forms a three-dimensional network trapping the oil and conferring appropriate performance to the oleogel. The physical, mechanical, and rheological properties of oleogels depend basically on the nature and concentration of its components, and the microstructure resulting from its manufacturing process.[2] Oleogels are received progressively considerable attention for use in a wide range of applications including foods, pharmaceuticals, separation science, and lubrication.[3–5] To act as a gelling agent, compounds need to fulfill certain physicochemical properties such as affinity for oil, surface activity, and self-assembling properties to form a colloidal network.[1] In this sense, different commodity plastics such as low-density polyethylene, high-density polyethylene, polypropylene (PP), or ethylene/vinyl acetate copolymer (EVA) might find a wide application in the industry as gelling agent and, consequently, it may create a new market niche with interesting perspectives in the future. However, very little work has been done using this approach. In previous works,[6,7] we reported a detailed study on the rheological, thermal, and mechanical properties of oleogels based on recycled polypropylene with mineral oil for a range of polymer concentration. From the results, it may be concluded that, these blends form systems, potentially applicable as lubricating greases. The evolution of the linear viscoelasticity functions with frequency was qualitatively similar to that found for traditional lithium lubricating grease with enhanced viscoelastic properties (e.g., storage modulus), with respect to this. Recently, we have also studied the influence of vinyl acetate (VAc) content on the rheological properties and microstructure of oleogels based on conventional and high-oleic sunflower vegetable oils and EVA copolymer. We found that VAc content and melt flow index of the EVA copolymer significantly affect the rheological and thermal responses of these systems.[8]

On the other hand, considerable research efforts have been aimed towards understanding the nonlinear viscoelastic (NLV) behavior of materials.[9] The investigation of NLV properties in materials presents a deep field of study, from the academic and industrial point of view. NLV properties are import in a number of diverse industrial manufacturing processes, e.g., extrusion, injection moulding, dough mixing, or film tentering.[9] NLV behavior may be observed at small strains for many systems such as suspensions,[10] gels,[11] emulsions,[12] and polymers.[13]

Table I. Some Physicochemical Characteristics of Polymers Used

	Density (g/cm^3)[a]	MFI (g/10 min)[b]	Melting point (°C)	M_w (g/mol)[c]	M_n (g/mol)[c]	M_w/M_n[c]	% VAc[d]
PP	0.905	12	165.8	5.71 10^4	2.89 10^4	1.97	–
EV18	0.937	500	83.6	3.52 10^4	1.64 10^4	2.15	18
EV28	0.950	400	71.8	4.07 10^4	1.91 10^4	2.12	28
EV34	0.956	45	62.2	6.02 10^4	2.96 10^4	2.03	34

[a] Supplied by manufacturers.
[b] Supplied by manufacturers refer to ASTM D1238 2.16 kg load at 190 °C for EVA samples, 2.16 kg load at 230 °C for PP sample.
[c] Determined by GPC.
[d] Supplied by manufacturers.

Nevertheless, it should be noted that, to the best of our knowledge, detailed studies on NLV properties of oleogel based on vegetable oils and polyolefins in shear flow are not available from literature. All works found in the bibliography on oleogels rheology are focused on: small amplitude oscillatory shear (SAOS) and steady state shear measurements.[1,3,4] Taking into account these considerations, the aim of this work was to study the linear (SAOS) and nonlinear (relaxation) measurements combined with polarized optical microscopy of new oleogels based on high-oleic sunflower oil (HOSO) and ethylene vinyl acetate copolymer (EVA) with different VAc content / isotactic polypropylene (iPP) blends.

EXPERIMENTAL

Material

iPP and three kinds of EVA commercially available, kindly supplied by Repsol S.A. (Spain) were used in this study. Table I provides characterization data such as density, melt flow index (MFI) and melting point as provided by Repsol. The number-average molecular weight (M_n), weight-average molecular weight (M_w), and polydispersity index (M_w/M_n) were determined by size exclusion gel permeation chromatography (GPC), using a GPC2000 Water apparatus. On the other hand, the VA content of the EVA copolymer was 18 wt % (EV18), 28 wt % (EV28), and 34 wt % (EV34), respectively. The VA content was provided by the supplier and the ratio was confirmed by TGA. The polymers were dissolved in a refined HOSO (density 0.9035 g/cm^3 at 25°C and a kinematic viscosity of 38 mm^2/s at 40°C with 85 wt % oleic acid) supplied by the Instituto de la Grasa, CSIC (Spain). It is composed of unsaturated linoleic (C18 : 2; 8.08 wt %) and oleic (C18 : 1; 83.66 wt %) acids as well as saturated stearic (C18 : 0; 4.42 wt %) and palmitic (C16 : 0; 3.84 wt %) fatty acids.

Manufacture of Oleogel Formulations

Processing of oleogels were performed in an experimental device known as "rheomixer" setup consisting of a cup (40 mm diameter, 71 mm height) and a stirring geometry (four-blade mixing head, 30 mm diameter) coupled with the transducer of a controlled-stress Haake RS600 rheometer (Germany). Vegetable oil/iPP polymer blends were prepared at 170°C. About 30 g of vegetable oil was stirred for 15 min at 400 rpm with the four-blade mixing geometry placed 12 mm above the bottom of the cylindrical vessel until the sample was thermostatized. Then, the iPP was added (2.5–7.5 wt %) to the mixing device and the

blend stirred for 1 h under the processing conditions previously established. After that EVA was added, at a concentration of 19 wt %, and blended for another 1 h, at the same conditions. Then, once a constant torque values were obtained, the oleogel was cooled down to room temperature on a 3–5 mm steel sheets in order to induce gelation. Vegetable oil/EVA blend was used as a control sample.

Rheological Measurements

A controlled-strain (ARES, TA Instruments, New Castle, USA) rheometer was used to study the rheology of oleogels, using a serrated plate-plate geometry, SPP (25 mm diameter, 1 mm gap), maintaining temperature at 25°C with a forced convection oven. Each test was run at least two replications with fresh samples. The viscoelastic linear region (LVR) was first determined by means of SAOS. In particular, strain amplitude sweep tests were performed, by applying the strain amplitude from $\gamma_o = 0.01\%$ to 600%, keeping a constant angular frequency of $\omega = 6.28$ rad/s. Once the linear viscoelastic region was determined, the mechanical spectra of the oleogels were obtained from SAOS frequency sweep tests. In the frequency sweep test a strain amplitude at $\gamma_o = 0.08\%$ was applied in all cases in a frequency range between $\omega = 100$ and 0.03 rad/s. Stress relaxation curves, in the linear and nonlinear viscoelasticity region were obtained by applying different constant strains, comprised between 0.08% and 200%. Stress relaxation modulus $G(t)$, which is defined as $G(t) = \tau(t)/\gamma_o$ was measured.

Microscopy

Optical microscopy observations were carried out with an Olympus BX52 (Japan) microscope with polarized light equipped with an Olympus C5050Z camera and an objective of 20×. Samples were carefully poured into a sample holder (76× 26 mm) and spread under the glass cover slip at room temperature.

RESULTS AND DISCUSSION

In Situ Monitoring the Rheological Properties During Mixing Process

The evolution of torque during mixing process of EV18-HOSO oleogels in a "rheomixer" as a function of iPP content is shown in Figure 1. All systems showed similar behavior. Three main processing stages can be observed in the figure. The first stage, from $t = 0$ to 10 min, where only vegetable oil was stirred to ensure that a constant temperature is reached. The second stage, from $t = 10$ to 70 min, is the iPP mixing zone. In this stage, the
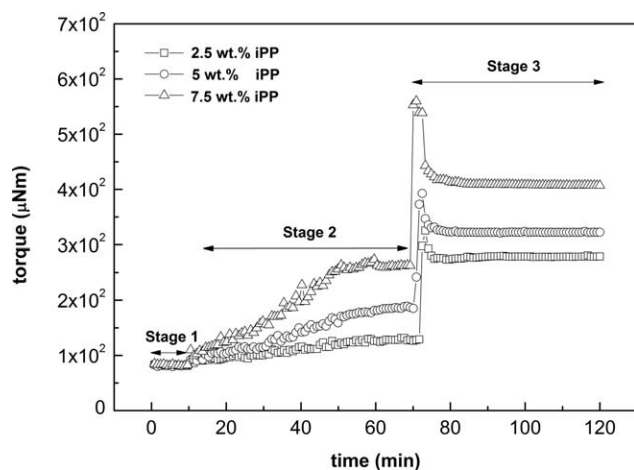
Figure 1. Evolution of torque with time during processing of EV18 oleogels with different PP content processing in a rheo-reactor, (■), PP = 2.5 wt %; (•), PP = 5 wt %; (▲), PP = 7.5 wt %.

iPP is introduced in the cup and the solid particles offer a certain resistance in a continuous oil phase to the rotation of the blades and therefore the torque increases. After a short time, when the heat transfer is sufficient to completely melt the solid particles, the torque exponential increases and reaches a steady-state regime. In this time, the polymeric domains interact with oil compounds and, as a consequence, an increase in the torque was observed for a relatively long time. The last stage, from $t = 70$ to 120 min, is the iPP/EVA blends mixing zone. The addition of EVA provokes a sudden sharp increase in the torque values, which is followed by a decline in torque values to reach a steady-state value after a certain time of mixing. As can be observed, the increase in mixing torque values is more gradual for iPP than EVA copolymer and the torque values increase with increasing in percentage of added iPP whilst the stationary torque value of oleogel with 7.5 wt % was ~32% higher than that of the oleogel with 2.5 wt % of iPP.

Linear Viscoelasticity Characterization

Oleogels were studied under oscillatory shear conditions, in order to define the upper limit of the linear viscoelastic range (Figure 2) and determine the mechanical spectrum (Figure 3) for each sample. Figure 2 shows storage and loss moduli dependence on strain amplitude. As long as the strain amplitude is small, G' and G'' curves present a constant plateau value. Here, the structure of the sample is only slightly perturbed, with it is viscoelastic response within the linear region. As can be observed, in all cases samples behave as gel-like materials ($G' > G''$) and the distance between moduli increases in a parallel form in the following order EV18-HOSO > EV28-
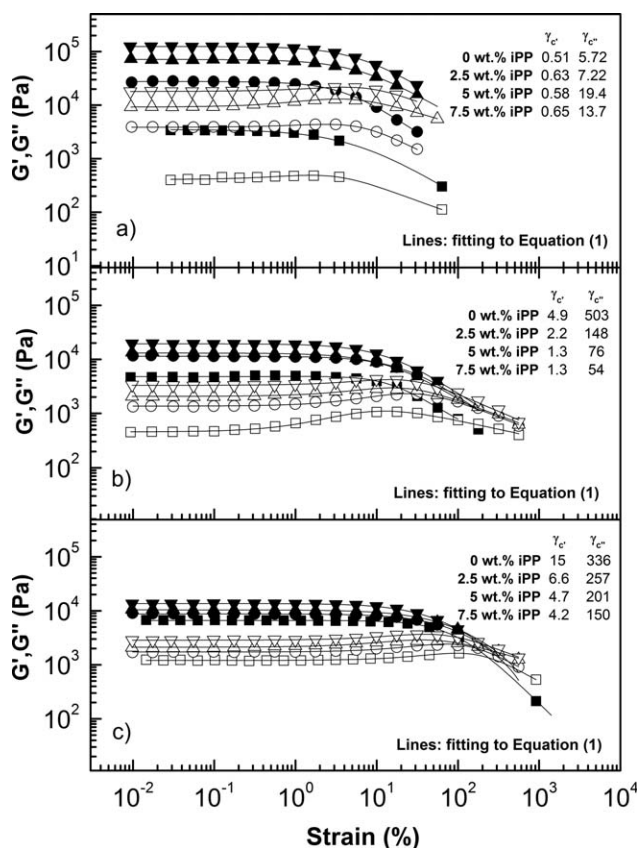

Figure 2. Oscillatory strain sweep tests at a constant frequency of $\omega = 6.28$ rad/s; closed symbol, G'; open symbol, G''; (■), PP = 0 wt %; (•), PP = 2.5 wt %; (▲), PP = 5 wt %; (▼), PP = 7.5 wt % for oleogels: (a) EV18, (b) EV28, (c) EV34. *Solid lines:* fitting to Equation (1).
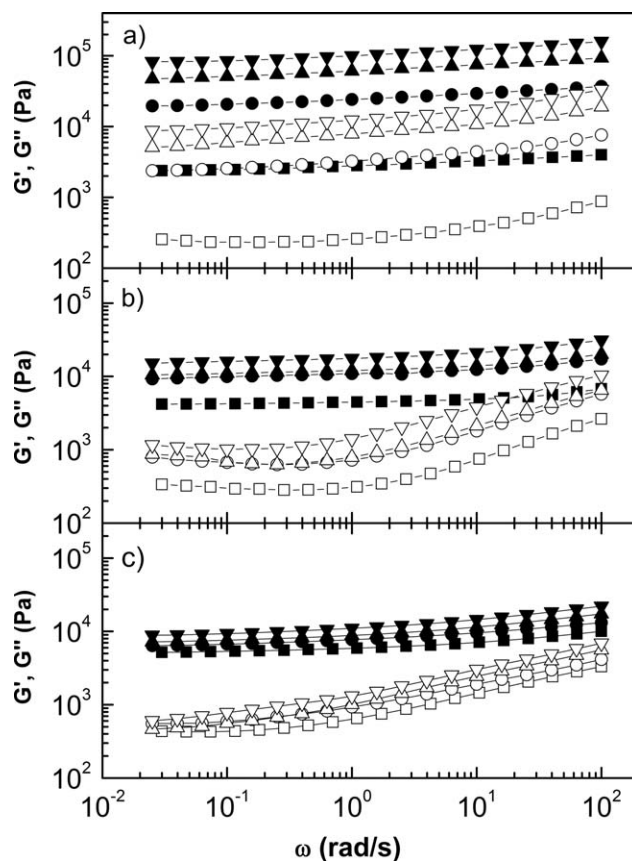

Figure 3. Frequency sweep tests at a constant strain of $\gamma_0 = 0.08\%$; closed symbol, G'; open symbol, G''; (■), PP = 0 wt %; (•), PP = 2.5 wt %; (▲), PP = 5 wt %; (▼), PP = 7.5 wt % for oleogels: (a) EV18, (b) EV28, (c) EV34.
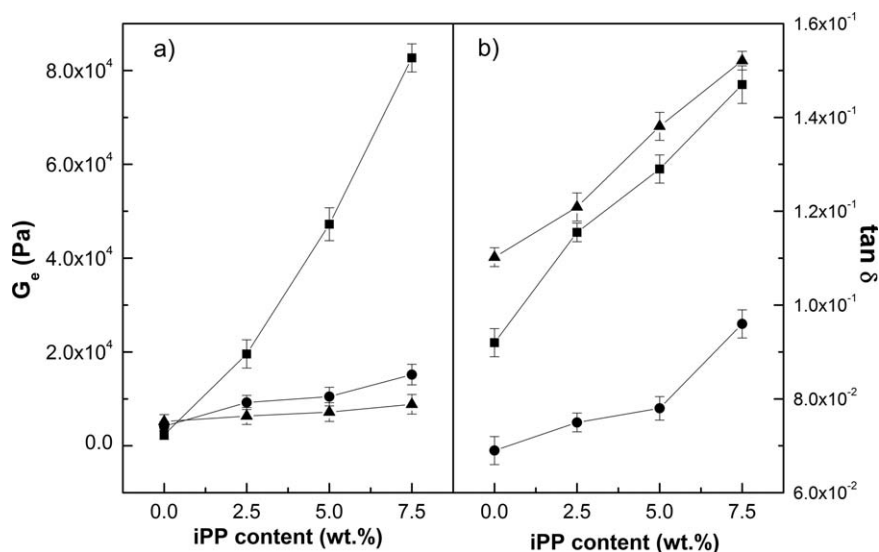
Figure 4. Evolution of the equilibrium elastic modulus, G_e (a) and loss tangent, tan δ (b) with PP content for oleogels: (■), EV18; (•), EV28 (▲), EV34.

HOSO > EV34-HOSO. This observation is because of the increasing elastic character of the oleogel response.[14] For all the oleogels, the storage modulus monotonically decreases with increasing strain, while the profile of the loss modulus shows a slightly increase at the end of the linear viscoelastic regime which is almost negligible for EV18-HOSO but evident for other oleogel (EV28-HOSO). This behavior is often exhibited by disperse systems and polymeric gels where particle concentration and/or interparticle attractive interactions or interchain associations show severe constraints to incipient flow of the relevant structural units such as particles, flocs, or gel microdomains.[14] The strain dependence of both moduli can be described by the following equation:[15]

$$G = G_o \frac{1 + a\gamma}{1 + b\gamma^n} \qquad (1)$$

where G_o represents the limiting values of the storage modulus and loss modulus in the linear viscoelastic regime, whereas a, b, n are adjustable parameters. The monotonic decay of the storage modulus implies that eq. (1) reduces to the Soskey–Winter equation ($a = 0$). The critical strain γ_c which represents limit of the LVR, can be arbitrarily associated with the condition $G = 0.95G_o$ and calculated from the equation parameters. Consequently, the critical strain values and the linear viscoelastic moduli can be derived from each system from simultaneous fitting of both experimental data series. The values of critical oscillatory strain (γ_c, $\gamma_{c'}$ for G' and G'', respectively) are shown in Figure 2. As can be observed, γ_c decreases as iPP content increases in all the oleogels, excepting oleogels with higher iPP content formulated with EV18. These values are typical of other systems like suspensions, polymer gels, and polymer solutions.

Figure 3 shows the evolution of linear viscoelasticity functions for EVA oleogels as a function of iPP content. The mechanical spectra obtained for these oleogels show an evolution of the storage (G') and loss (G'') moduli with frequency that is typical of polymeric systems with physical entanglements,[16] being qual-

itatively similar for all the oleogels studied. This behavior is also similar to those obtained for amorphous /recycled iPP-based gel-like dispersions.[7] The mechanical spectrum presents the so called "plateau" region that is characterized by a slight frequency dependence for G' and a minimum in G''. Occurrence of this plateau region is related to the formation of physical entanglements in polymeric materials.[17] In this case, it may be attributed to the colloidal gel network formed by EVA and iPP polymers, respectively. These systems obey the definition of gel where $G' > G''$ with both moduli showing some significant frequency dependence at low frequencies and elastic equilibrium modulus, G_e, can be defined:[18]

$$G_e = \lim_{\omega \to 0} G' \qquad (2)$$

Figure 4 shows the values of the equilibrium modulus (G_e) and the loss tangent (tan $\delta = G'/ G''$) at 1 rad/s obtained for EVA oleogels as a function of iPP content. As may be seen in Figure 4, G_e always presents an increase with iPP content showing more remarkable increase for oleogels formulated with EV18. On the other hand, the values obtained for tan δ are higher for oleogels formulated with EV18 and EV34, showing a more viscous character than EV28-HOSO based oleogels. This behavior may be related to the higher viscosity of EV34 and EV18 polymer phase, as it has reported in previous work.[8]

Nonlinear Viscoelasticity Characterization
NLV properties for the oleogels were studied by shear stress relaxation tests outside the linear viscoelastic regime. The influence of the applied strain on the relaxation modulus $G(\gamma,t)$ was studied through stress relaxation tests. Figure 5 displays the evolution of the nonlinear relaxation modulus, $G(\gamma,t)$, at different applied strains for oleogels formulated with EV18 (a), EV28 (b) and EV34 (c), as well as the reference linear relaxation modulus. As shear strain is increased, $G(\gamma, t)$ decreases with strain. Furthermore, log (G) versus log (t) plots follows a power law decay in the experimental range studied and its slope is almost
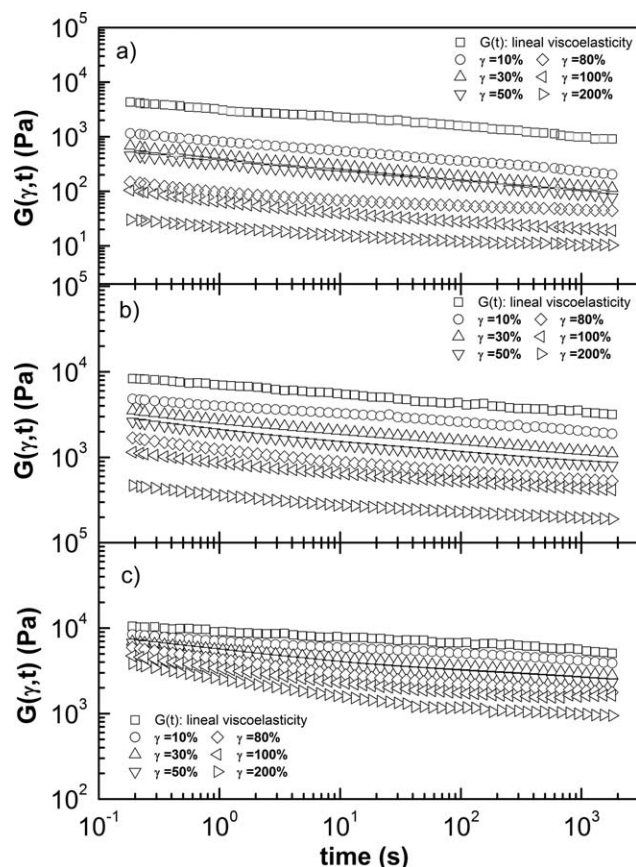
Figure 5. Time-dependent nonlinear stress relaxation modulus $G(t, \gamma)$ at different strain $\gamma = 0.08$ (lineal viscoelasticity), 10, 30, 50, 80, 100, 200% for oleogels: (a) EV18, (b) EV28, (c) EV34.

independent of the strain applied to the sample. As a consequence, it may be suggest that the oleogels studied obey the time-strain factorability, so that the nonlinear shear relaxation modulus $G(\gamma, t)$ can be separated into two components: a time dependent function, the linear relaxation modulus, $G(t)$, and strain-dependent function, the so-called "damping function", $h(\gamma)$. This factorability is therefore expressed by

$$G(\gamma, t) = G(t) \cdot h(\gamma) \quad (3)$$

This time-strain factorability has been previously used for entangled polymer systems,[19] lithium lubricating greases modified with reactive polymers[20] or oil-in-water emulsions.[12] The damping function is a rheological parameter that can be used to evaluate the structural resistance of oleogels under shear, although, in this case, at constant applied strain. Figure 6 shows the values of the damping function calculated from eq. (3), for the oleogels studied as a function of iPP content. As can be observed, the values and the evolution of the damping function are quite similar for all the oleogels studied. In this sense, a dramatic decrease in the values of this function in the NLV region is always noticed, even at relatively low values of the applied strain (10%). This fact reveals a remarkable strain softening behavior for oleogels studied, compared to the behavior found for entangled polymer systems. Consequently, nonlinearity appears at smaller deformations than that predicted with entangled polymer solutions (i.e. the Doi–Edwards tube model

theory for entangled linear polymers[21] or the force-balanced network model by Marrucci et al.[22] The evolution of the damping function is well described by the Soskey–Winter empirical model:[23]

$$h(\gamma) = \frac{1}{1 + a\gamma^b} \quad (4)$$

where a and b are dimensionless parameters, related to the materials functions. The values of parameter "a" and "b" are collected in Table II for the oleogels studied. The values found for parameter "b" are 1.16 ± 0.20 in all cases (see Table II), and consequently, this parameter may be fixed for the sake of simplicity ($R^2 > 0.950$). As can be observed in oleogel without iPP, the value of parameter "a" is higher for EV18-HOSO oleogel, and then decreases for EV28-HOSO and EV34-HOSO. This is indicative of a larger influence of deformation on EV18-HOSO oleogel. This means that the microstructure of these oleogels was more affected by the deformation when VAc content decreases in EVA copolymer. Hence, the linear relaxation modulus shows the smallest values for EV18-HOSO oleogel and its microstructure is more easily destroyed by applying a deformation outside the linear viscoelastic region. For all oleogels, the value of parameter "a" increases with iPP content. This means that the microstructure developed in oleogel was more strongly affected by the deformation at higher iPP content. This

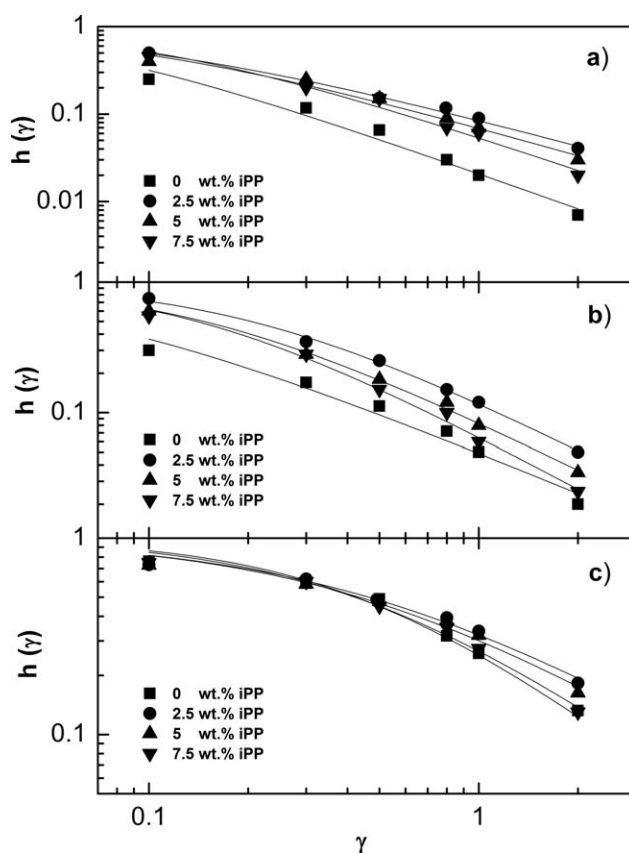
Figure 6. Evolution of the damping function $h(\gamma)$ with shear strain; (■), PP = 0 wt %; (•), PP = 2.5 wt %; (▲), PP = 5 wt %; (▼), PP = 7.5 wt % for oleogels: (a) EV18, (b) EV28, (c) EV34. *Solid lines:* fitting to a Soskey–Winter model.

Table II. Values for the Parameters of the Soskey–Winter Model for Oleo-gels Studied

	wt % PP	A	b
EV18	0	47.4 ± 8.4	1.34 ± 0.16
	2.5	10.9 ± 0.39	1.03 ± 0.04
	5	13.6 ± 0.99	1.08 ± 0.08
	7.5	17.8 ± 1.39	1.27 ± 0.08
EV28	0	19.5 ± 2.19	1.05 ± 0.10
	2.5	7.63 ± 0.23	1.27 ± 0.04
	5	11.1 ± 0.39	1.25 ± 0.04
	7.5	14.5 ± 0.81	1.36 ± 0.07
EV34	0	2.95 ± 0.16	1.26 ± 0.08
	2.5	2.11 ± 0.11	0.97 ± 0.07
	5	2.32 ± 0.14	1.01 ± 0.08
	7.5	2.76 ± 0.15	1.17 ± 0.08

behavior could be attributable to strain-induced disruption of the network structure formed by the iPP in EVA phase.

Morphology Analysis

Optical characterization was performed in order to determine the morphology of oleogels. Polymer gel network forms an interconnected three-dimensional sponge-like structure with crystalline and amorphous fractions of polymer, yielding a gel-type morphology, which would remain stable at temperatures below the melting point.[8] This polymer network is responsible for the rheological behavior, in which the systems exhibited predominantly elastic properties. The crystalline fraction was observed by using optical microscopy with polarized light. Figure 7 shows selected micrographs of oleogels with 5 wt % iPP content, at a magnification of·20×. As can be observed, oleogel modified with iPP yields a new phase in the oleogels, as may be deduced from optical microscopy observations, where two different polymer phases are clearly displayed. The lightly toned regions are assigned to a polymer-rich phase, whereas the oil-rich phase appears dark. In all cases, EVA copolymer phase appears as tiny distributed crystals that tend to fill the whole space [Figure 7(a)], while iPP appears as large typical birefringent alpha phase negative spherulites[24] dispersed in the EVA copolymer phase which under observation conditions appear completely crystallized. In addition, for EV18-HOSO oleogel, same independent polymer particles, with around radius of 10 µm are dispersed within the oleogel matrix, acting as filler in the oleogel matrix. This morphology would give, as a result, a higher linear viscoelasticity functions.

CONCLUSIONS

This work presents a study of the (linear and nonlinear) viscoelasticity behavior and morphological analysis of oleogels based on HOSO and EVA copolymer with different VAc content / iPP blends. Oleogels were prepared by using the mixing rheometry technique in a batch mixer. Three different zones subsequently related to polymer addition, dispersion and further blending could be distinguished. The increase in mixing torque values was more gradual for iPP than EVA copolymer and the torque

values increased with addition of iPP. The results obtained during the oscillatory strain amplitude sweep tests confirmed that the limit of the LVR lies at low strains. The end from linearity for oleogels were accompanied by opposite trends for G' and G'', while the storage modulus monotonically decreases with increasing strain, the profile of the loss modulus shows a slightly increase which is almost negligible for EV18-HOSO but evident for EV28-HOSO oleogels. The evolution of the linear viscoelasticity functions with frequency is typical of polymeric
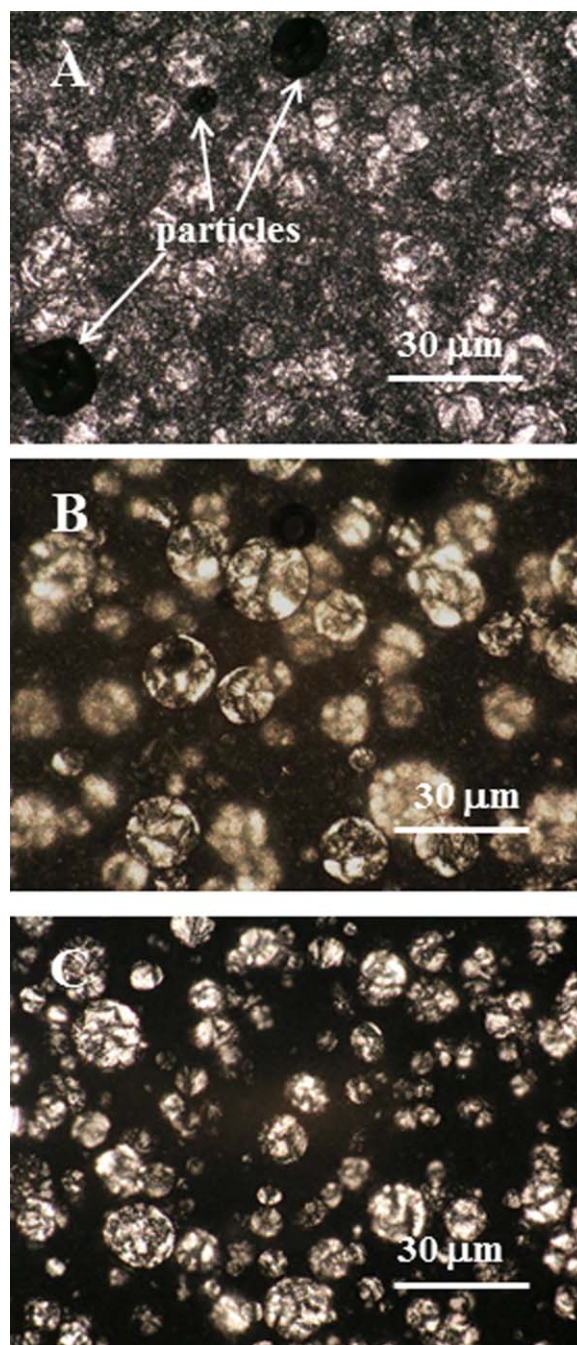

Figure 7. Polarized-light optical microscopy images for oleogels with 5 wt % PP: (a) EV18; (b) EV28; (c) EV34. [Color figure can be viewed in the online issue, which is available at wileyonlinelibrary.com.]

systems with physical entanglements being qualitatively similar for all the oleogels. It was observed that the elastic equilibrium modulus and loss tangent increases with iPP content. Regarding the NLV behavior, oleogels showed a strong dependence on the strain applied with NLV behavior evidenced at strains above 10%. The damping function was evaluated from stress relaxation data with the Soskey–Winter empirical model being found to provide a fairly well description of the nonlinear behavior of these oleogels.

In summary, these results show that, the content of iPP in oleogels and VAc in EVA copolymer exert much influence on linear and NLV properties of oleogels. This finding may be of interest in the design of oleogles having controlled rheological properties.

ACKNOWLEDGMENTS

NOMENCLATURE

G'	storage modulus (Pa)
G''	loss modulus (Pa)
G_e	equilibrium modulus (Pa)
G	relaxation modulus (Pa)
a, b	Soskey–Winter damping factors
h	damping function
t	time (s)
M	torque (µNm)
$\tan \delta$	loss tangent
LVR	viscoelastic linear region
NLV	nonlinear viscoelastic
SPP	serrated plate-plate

Greek letters

γ	strain (per cent)
$\gamma_{c'}$	critical oscillatory strain of the G' (per cent)
$\gamma_{c''}$	critical oscillatory strain of the G'' (per cent)
ω	angular frequency (rad/s)
λ	relaxation time (s)

REFERENCES

1. Patel, A. R.; Schatteman, D.; De Vos, W. H.; Lesaffer, A.; Dewettinck, K. *J. Colloid. Inter. Sci.* **2013**, *411*, 114.

2. Martín-Alfonso, J. E.; Romero, A.; Valencia, C.; Franco, J. M. *J. Ind. Eng. Chem.* **2013**, *19*, 580.

3. Behera, B.; Patil, V.; Sagiri, S. S.; Pal, K.; Ray, S. S. *J. Appl. Polym. Sci.* **2012**, *125*, 852.

4. Núñez, N.; Martín-Alfonso, J. E.; Valencia, C.; Sánchez, M. C.; Franco, J. M. *Ind. Crops Prod.* **2012**, *37*, 500.

5. Toro-Vazquez, J. F.; Morales-Rueda, J.; Mallia, V. A.; Weiss, R. G. *Food Biophys.* **2010**, *5*, 193.

6. Martín-Alfonso, J. E.; Valencia, C.; Arteaga, J. F.; Díaz, M. J.; Franco, J. M. *J. Appl. Polym. Sci.* **2013**, *127*, 1369.

7. Martín-Alfonso, J. E.; Valencia, C.; Franco, J. M. *Polym. Test.* **2013**, *32*, 516.

8. Martín-Alfonso, J. E.; Franco, J. M. *Polym. Test.* **2014**, *37*, 78.

9. Carriere, C. J.; Inglett, G. E. *Food Hydrocoll.* **2003**, *17*, 605.

10. Uematsu, H.; Aoki, Y.; Sugimoto, M.; Koyama, K. *Rheol. Acta* **2010**, *49*, 1187.

11. Pham, K. N.; Petekidis, G.; Vlassopoulos, D.; Egelhaaf, S. U.; Pusey, P. N.; Poon, W. C. K. *J. Rheol.* **2008**, *52*, 649.

12. Bengoechea, C.; Puppo, M. C.; Romero, A.; Cordobés, F.; Guerrero, A. *J. Food Eng.* **2008**, *87*, 124.

13. Sugimoto, M.; Suzuki, Y.; Hyun, K.; Ahn, K. H.; Ushioda, T.; Nishioka, A.; Taniguchi, T.; Koyama, K. *Rheol. Acta* **2006**, *46* 33.

14. Lawal, O. S.; Lapasin, R.; Bellich, B.; Olayiwola, T. O.; Cesàro, A.; Yoshimura, M.; Nishinari, K. *Food Hydrocoll.* **2011**, *25*, 1785.

15. Lapasin, R.; Grassi, M.; Coceani, N. *Rheol. Acta* **2001**, *40*, 185.

16. Ferry, J. D. Viscoelastic Properties of Polymers; Wiley: New York, **1980**.

17. Gupta, R. K. Polymer and Composite Rheology; Marcel Dekker: New York, **2000**.

18. Barral, M. S.; Muñoz, M. E.; Santamaría, A. *Rheol. Acta* **2001**, *40*, 193.

19. Archer, L. A.; Juliani. *Macromolecules* **2004**, *37*, 1076.

20. Moreno, G.; Franco, J. M.; Valencia, C.; Gallegos, C. *J. Appl. Polym. Sci.* **2010**, *118*, 693.

21. Doi, M.; Edwards, S. F. The Theory of Polymer Dynamics; Oxford University: New York, **1986**.

22. Marrucci, G.; Greco, F.; Ianniruberto, G. *J. Rheol.* **2000**, *44*, 845.

23. Soskey, P. R.; Winter, H. H. *J. Rheol.* **1984**, *28*, 625.

24. Chen, J. H.; Chang, Y. L. *J. Appl. Polym. Sci.* **2007**, *15*, 1093.